J. Wind Eng. Ind. Aerodyn. 104-106 (2012) 360–368

Contents lists available at SciVerse ScienceDirect

Journal of Wind Engineering and Industrial Aerodynamics

journal homepage: www.elsevier.com/locate/jweia

RANS simulation of ABL flow over complex terrains applying an Enhanced k-ε model and wall function formulation: Implementation and comparison for fluent and OpenFOAM

M. Balogh [a,*], A. Parente [b], C. Benocci [c]

[a] Department of Fluid Mechanics, Budapest University of Technology and Economics, Budapest, H-1111 Budapest, Bertalan Lajos u. 4-6, Hungary
[b] Service d'Aéro-Thermo-Mécanique, Université Libre de Bruxelles, Bruxelles, Belgium
[c] Environmental and Applied Fluid Dynamic Department, Von Karman Institute for Fluid Dynamics, Rhode-St-Genèse, Belgium

ARTICLE INFO

Available online 1 April 2012

Keywords::
RANS
ABL
CFD simulation
Enhanced k-ε model
Complex terrain

ABSTRACT

The simulation of Atmospheric Boundary Layer (ABL) flows is commonly performed using commercial CFD codes with RANS turbulence modeling, applying the standard k-ε model. However, when applied to the simulation of the homogenous ABL, this approach may result in an undesired decay of the velocity and turbulent fully–developed profiles specified at the inlet of the computational domain. This behavior is due to an inconsistency between turbulence model, inflow conditions and wall function formulation. An approach has been introduced recently to overcome this problem, which consists in the modification of the turbulence model and wall function formulation to retrieve an overall consistent treatment of the neutral ABL. Such methodology, previously applied to simulation of the atmospheric boundary layer over flat terrain and ground-mounted bluff bodies, is here applied to the simulation of the flow over complex terrains and hills, at wind tunnel and atmosphere scale. In a time of limited scientific funding, the availability of open source CFD software such as OpenFOAM is a very attractive option to investigate; therefore, a comparison between OpenFOAM and the commercial code FLUENT 13.0 has been carried out in the present paper. The potential of the proposed methodology and the satisfactory performances of OpenFOAM are demonstrated.

1. Introduction

The simulation of atmospheric flows over complex terrains is necessary for the estimation of wind load on buildings as well as for the choice of sites for windmills and wind farms. This topic has been intensively investigated by several research groups (e.g. Castro et al., 2003a, 2003b; Bechmann, 2006; Bechmann et al., 2009; Blocken et al., 2007a, 2007b) The major part of the available investigations was performed by means of Reynolds-Averaged Navier-Stokes (RANS). Large Eddy Simulation (LES) studies of ABL flows (Shah and Ferziger, 1997; Bechmann, 2006; Bechmann et al., 2009; Xie and Castro, 2006; Crasto, 2007; Lim et al., 2009; Dejoan et al., 2010) can provide a more accurate solution for the turbulent flow field with respect to RANS simulations, provided that the range of resolved turbulent scales is sufficiently large and that the inflow conditions are well characterized. However, LES simulations are significantly more expensive than RANS (Rodi, 1997) and, therefore, practical simulations of ABL flows are still often carried out using RANS in combination with two-equation turbulence models, to provide fast answers to design questions. Indeed, for this approach to be effective, turbulence modeling should adequately describe the problem under investigation.

However, the application of two-equation RANS turbulence models with standard rough wall functions often results in unsatisfactory predictions, due to an inconsistent formulation of the law of the wall for rough surfaces and the fully developed inlet conditions for ABL simulations (Richards and Hoxey, 1993; Blocken et al., 2007a, 2007b; Franke et al., 2007; Gorlé et al., 2009; Parente et al., 2011a). In a recent work, Parente et al. (2011b) proposed a new approach ensuring consistency among turbulence model, inlet and wall boundary conditions for the numerical simulation of neutral ABL flows. This is accomplished through a reformulation of the wall function based on the aerodynamic roughness and on the derivation of the kinetic energy inlet profile from the solution of the turbulent kinetic energy transport equation. Such an approach has been validated for the simulation of a homogeneous neutral ABL and a ground mounted bluff body using the commercial CFD code Fluent (Parente et al., 2011b).

In the present work, the approach has been adapted for the simulation of flows above complex terrains. Moreover, a benchmark between the commercial code Fluent and the open-source software OpenFOAM has been carried out. This is of interest because of the increasing use of OpenFOAM within the scientific

* Corresponding author. Tel.: +36 360 6925; fax: +36 1 463 3464.
E-mail address: baloghm@ara.bme.hu (M. Balogh).

0167-6105/$ - see front matter © 2012 Elsevier Ltd. All rights reserved.
doi:10.1016/j.jweia.2012.02.023

community. The proposed method is validated against experimental data for a homogenous 2D boundary layer (Donat, 1995) and applied to a wind-tunnel scale 3D hill model (Takahashi et al., 2005) as well as to a full-scale case, the Askervein Hill (Taylor and Teunissen, 1983, 1985, Mickle et al., 1988).

In the present paper, the new modeling methodology is compared to standard modeling approaches, demonstrating the validity of the approach.

In the second section of the present paper the theoretical basis of the new approach are be introduced, including the proposed modifications of the wall function and turbulence model. Some implementation details are given in the third section, for both OpenFOAM and Fluent, including their numerical settings. In the fourth section, the application cases of the new approach together with the results of the simulations are detailed and discussed.

2. Governing equations and models

Applying the standard k-ε model, the RANS equations for homogeneous, neutral atmospheric boundary layers can be written in the following 1D form assuming constant pressure and shear stress, and zero vertical velocity:

$$\nu_t \frac{\partial u}{\partial z} = \frac{\tau_w}{\rho} = u_\tau^2 \tag{1}$$

$$\frac{\partial}{\partial z}\left(\frac{\nu_t}{\sigma_\varepsilon}\frac{\partial k}{\partial z}\right) + G_k - \varepsilon = 0 \tag{2}$$

$$\frac{\partial}{\partial z}\left(\frac{\nu_t}{\sigma_\varepsilon}\frac{\partial \varepsilon}{\partial z}\right) + C_{\varepsilon 1} G_k \frac{\varepsilon}{k} - C_{\varepsilon 2}\frac{\varepsilon^2}{k} = 0 \tag{3}$$

where τ_w is the wall shear stress, u_τ is the corresponding friction velocity, k and ε are respectively the turbulent kinetic energy and its dissipation, G_k denotes the production of the turbulent kinetic energy and ν_t is the kinetic eddy viscosity, which are written as:

$$G_k = \nu_t\left(\frac{\partial u}{\partial z}\right)^2, \quad \nu_t = C_\mu \frac{k^2}{\varepsilon} \tag{4}$$

σ_k, σ_ε, $C_{\varepsilon 1}$, $C_{\varepsilon 2}$, C_μ are the coefficients of the standard k-ε model, whose values are generally fixed as 1.0, 1.3, 1.44, 1.92, and 0.09 respectively. However, the application of those standard values to the simulation of the neutral ABL results in an inconsistent formulation (Richards and Hoxey, 1993) and modifications need to be performed to obtain a consistent set of equations, as discussed in the following.

2.1. Modified wall treatments

The limitations related to the RANS simulation of neutral atmospheric boundary layer (ABL) with commercial CFD codes are due to an inconsistency between the wall function formulation and the fully developed inflow conditions for ABL (Riddle et al., 2004; Franke et al., 2007; Blocken et al., 2007a, b; Hargreaves and Wright, 2007). Remedial measures have been proposed in the literature (Blocken et al., 2007b); however, these are generally code dependent and they do not provide a general solution to the problem. In particular, such modifications only affect the velocity profile and the effect of roughness on turbulent quantities is not taken into account, causing an undesired non-homogeneity of the turbulent quantities throughout the computational domain.

A new approach has been recently proposed (Parente et al., 2011a), which addresses and solves the problem. This approach specifies velocity, turbulent kinetic energy and its dissipation rate in the wall adjacent cell using a formulation consistent with the velocity and turbulence inlet profiles. Assuming logarithmic profiles for the velocity, the dissipation ε_p and the production term G_k for k_p at first inner node (z_p) are reformulated following Eq. (5), where the subscript p indicates the cell value of the quantity at the wall adjacent cell, while z_0 is the aerodynamic roughness

$$u_p = \frac{u_\tau}{\kappa}\ln\left(\frac{z_p+z_0}{z_0}\right), \quad \varepsilon_p = \frac{C_\mu^{0.75}k_p^{1.5}}{\kappa(z_p+z_0)}, \quad G_k = \frac{\tau_w^2}{\kappa C_\mu^{0.25}k_p^{0.5}(z_p+z_0)}. \tag{5}$$

It can be observed that, differently from Richards and Hoxey (1993), the production of turbulent kinetic energy at the wall is computed at a location displaced by the aerodynamic roughness, z_p+z_0, to ensure consistency with turbulent dissipation rate calculation. In Parente et al. (2011a) this formulation was proved to be effective in removing the peak of turbulent kinetic energy observed at the wall (Hargreaves and Wright, 2007).

As far as the numerical implementation is concerned, the form of the universal law of the wall is preserved, i.e. $u_p = u_\tau/\kappa\ \ln(E' z_p^{+'})$, through the introduction of a new wall function constant and the non-dimensional wall distance as $E' = \nu/(z_0 u_\tau)$ and $z_p^{+'} = u_\tau (z_p^+ + z_0)/\nu$. The non-dimensional distance $z^{+'}$ is simply a z^+ shifted by the aerodynamic roughness, whereas the new wall function constant depends on the roughness characteristics of the surface. The friction velocity is calculated locally as $u_\tau = C_\mu^{0.25}\ k_p^{0.5}$.

The wall function based on the aerodynamic roughness is compared to an alternative wall function formulation based on the approach proposed by Blocken et al. (2007a). The latter is derived by imposing first-order matching between the inlet velocity profile and the velocity imposed by the wall function at the wall adjacent-cell. In particular, under the assumption that regime is fully rough, the roughness constant is computed using the physical roughness as $C_s = Ez_0/(0.95(z_p+z_0))$ where the equivalent sand grain roughness is set to $K_s = 0.95 z_p$, hence

$$u_p = \frac{u_\tau}{\kappa}\ln\left(\frac{z_p+z_0}{z_0}\right) = \frac{u_\tau}{\kappa}\ln\left(\frac{Ez_p^+}{1+C_s K_s^+}\right) \xrightarrow{1 \ll C_s K_s^+} C_s = \frac{Ez_0}{0.95(z_p+z_0)}. \tag{6}$$

This latter version of the rough wall function will be indicated as original wall function approach (denoted by O) in the following, using the values proposed by Richards and Hoxey (1993) for turbulent kinetic energy production, G_k, and turbulent dissipation rate, ε_p.

2.2. Modifications on the k-ε turbulence model

The inlet boundary conditions proposed by Richards and Hoxey (1993) are widely used for simulating the neutral ABL:

$$u = \frac{u_\tau}{\kappa}\ln\left(\frac{z+z_0}{z_0}\right), \quad \varepsilon = \frac{u_\tau^3}{\kappa(z+z_0)}, \quad k = \frac{u_\tau^2}{C_\mu^{0.5}}. \tag{7}$$

The boundary conditions in Eq. (7) automatically satisfy the 1-D momentum and k-ε equations, if the turbulent Prandtl number of the dissipation rate is expressed as $\sigma_\varepsilon = \kappa^2/((C_{\varepsilon 2} - C_{\varepsilon 1})C_\mu^{0.5})$. This formulation is equivalent (Parente et al., 2011a) to using the standard σ_ε value of 1.3 and applying an additional source term in the transport equation of turbulent dissipation rate (S_ε), as proposed by Pontiggia et al. (2009).

More realistic boundary conditions were proposed by Yang et al. (2009) for the turbulent kinetic energy, which takes the form $k = (A\ \ln(z+z_0)+B)^{0.5}$. Gorlé et al. (2009) proposed a modification of the constant C_μ and of the turbulent dissipation Prandtl number, σ_ε, which provided an approximate solution to the system of equations when using the inlet profile of Yang et al. (2009). In addition to that, Parente et al. (2011a) introduced two

source terms in the transport equations for k and ε, respectively, to guarantee an exact solution to the model equations when using these inlet profiles.

More recently, Parente and Benocci (2010) developed a comprehensive approach for the numerical simulation of neutral ABL flows. A novel profile for turbulent kinetic energy was derived from the solution of the turbulent kinetic energy transport equation, resulting in a new set of fully-developed inlet conditions for the neutral ABL. The consistency between the inlet profiles and the standard k-ε model was ensured with the introduction of a universal source term in the transport equation for the turbulent dissipation rate, ε, and the re-definition of the coefficient C_μ as a wall distance dependent value: $C_\mu = u_\tau / (A\ln(z+z_0)+B)$. The overall approach (Parente et al., 2011b) was proved to be successful for the simulation of unperturbed ABL using Fluent, but inadequate for separated regions. To overcome this drawback, the concept of Building Influence Area was adopted (*BIA*), following Gorlé et al. (2010), to allow a gradual transition of the turbulence model parameters from the values compatible with the unperturbed ABL to the ones adequate for the regions perturbed by the presence of obstacles. In this approach, the departure from the undisturbed flow conditions was measured locally by evaluating the deviation of the actual local velocity profile from the inlet logarithmic one. A blending function between the standard k-ε model values and the proposed ABL formulation was proposed for C_μ and the k source terms as:

$$C_\mu^{Blended} = 0.09 + (C_\mu - 0.09)(1 - f_{error})^N, \quad S_\varepsilon^{Blended} = S_\varepsilon (1 - f_{error})^N \tag{8}$$

where N is the blending exponent, 0.09 represents the standard value of the k-ε model parameter C_μ. The error function is defined as:

$$f_{error} = \frac{|U - U_{ref}|}{|U_{ref}|} \tag{9}$$

where U_{ref} denotes the undisturbed reference velocity vector.

In the present paper, the latter approach was implemented in OpenFOAM, with the specific purpose of improving the *BIA* concept for flows over complex terrains.

The entire present approach was thought and implemented on the standard formulation of k-ε model, but it is also compatible with the different modifications to the standard k-ε model proposed in the literature (Launder and Kato, 1993; Yap, 1987; Tsuchiya et al., 1997) to improve the simulation of separation and reattachment regions. As the research was aimed to the simulation of atmospheric flows over hilly terrain or building blocks, these modifications were implemented and tested to attempt to improve the simulation and to assess their influence on the results. The Kato-Launder approach is based on the reformulation of the production term written as

$$P_k^{STD} = \nu_t S^2 \quad \text{vs.} \quad P_k^{KL} = \nu_t S \Omega \tag{10}$$

where S is the modulus of the rate of strain tensor (symmetric part of the velocity gradient tensor) and Ω is the vorticity (antisymmetric part of the velocity gradient tensor). The approach proposed by Yap is a correction for separated flows; it corrects the turbulent kinetic energy prediction in the separated regions through an additive source term in the ε transport equation, defined as:

$$S_\varepsilon^{Yap} = 0.83 \frac{\varepsilon^2}{k} \left(\frac{k^{1.5}}{\varepsilon l_e} - 1 \right) \left(\frac{k^{1.5}}{\varepsilon l_e} \right)^2 \tag{11}$$

where $l_e = C_\mu^{-0.75} \kappa\, d_w$, and d_w is the nearest wall distance. The Yap correction is applied together with the Kato-Launder approach, as it is suggested by Launder (1993), thus it is hereafter denoted as KLY.

The modification proposed by Tsuchiya et al. (usually reported as MMK model in the literature) differs from the standard k-ε model by the evaluation of the eddy viscosity ν_t. In this approach, the standard formulation of ν_t is modified by a multiplier expressed as a constrained ratio between the vorticity and the modulus of the rate of strain tensor:

$$F_{MMK} = \min\left(\frac{\Omega}{S}, 1 \right) \rightarrow \nu_t = F_{MMK} C_\mu \frac{k^2}{\varepsilon} \tag{12}$$

3. Implementation and numerical methods

3.1. OpenFOAM

The approach and the model improvements discussed in the previous section were implemented in OpenFOAM. All the wall function treatments and the source terms for turbulent dissipation rate are included in the Reynolds-Averaged Navier-Stokes (RANS) module of the code, following the description given in Section 2. To respect the structure of the code, a new turbulence model is defined and denoted as ABL k-ε model. All of the modifications are available as options, which can be activated within the RANS model properties, which uses the setup file called RASProperties in OpenFOAM. The case selectors are vectors with three digital components (i, j, k) spanning the options summarized in Table 1. For example, the model applied as the standard k-ε model, if all selectors are set to zero except $P_{k,sel} = (1, 0, 0)$ and $C_{\mu,sel} = (1, 0, 0)$.

3.2. Ansys-fluent

The implementation of the new approach in Fluent is more complicated than in OpenFOAM, since the manipulation of the models is not straightforward. The modifications are performed by means of User Defined Functions (UDF). As the implementation of the standard k-ε model makes impossible to set C_μ as a local parameter, the realizable k-ε model was used to implement the approach discussed in Section 2, as it already takes into account a variable C_μ. The model is first converted to a standard k-ε model and then it is generalized to match the ABL k-ε model formulation. Importantly, the definition of the eddy viscosity according to the realizable k-ε model is overwritten by introducing a user-specified turbulent. The implementation in Fluent resembles the OpenFOAM implementation as much as possible. However, a perfect consistency cannot be guaranteed, as Fluent does not provide access to the source code, thus the details of the implementation might be different.

3.3. Numerical setup

To allow a meaningful comparison between Fluent and OpenFOAM, the numerical settings have been selected to be as similar as possible.

In this work, all the OpenFOAM simulations were carried out with the *simpleFoam* solver, which is a steady state, incompressible

Table 1
Switching options of the ABL k-ε model.

Selector	Option for	i value	j value	k value
ε_{sel}	ε source term	for arbitrary inlet	Yap correction	blending on
M_{sel}	model version	G_k of STD k-ε	G_k of KL k-ε	ν_t of MMK k-ε
$C_{\mu\ sel}$	C_μ value	0.09	homogeneous ABL	blending on

solver. For the spatial discretization of differential operators, the Gaussian integration was used with different interpolation schemes. The 2nd order linear interpolation was applied for gradient terms, the 2nd order upwind interpolation for divergence terms, while for the Laplacian terms the 2nd order linear interpolation was used with explicit non-orthogonal correction. The preconditioned conjugate gradient solver was applied with simplified diagonal-based incomplete Cholesky preconditioner for pressure, and its bi-conjugate version with incomplete LU preconditioner for velocity and turbulence. The SIMPLE method was used for pressure-velocity coupling. The relaxation parameters were set to the default value of 0.3 for pressure and of 0.7 for the other prognostic variables.

In Fluent simulations, the second order upwind schemes were used for velocity and turbulence, and the second order scheme is applied for pressure. Some numerical simulations presented divergence when the SIMPLE method for pressure-velocity coupling was employed. Therefore, the coupled scheme was used to avoid this problem, with the explicit under-relaxation factors of 0.75 for both the momentum and pressure. For the turbulent quantities, a value of 0.8 for the under-relaxation factors appeared satisfactory for reaching the full convergence.

4. Results and discussion

The approach and the model improvements discussed in the second section are tested and validated on three different cases with increased complexity. The homogeneous ABL approach was simulated on a simple empty fetch at laboratory scale, while its adaptation for hilly terrain is validated on a sinusoidal hill at laboratory scale and, on the Askervein hill at full scale. The settings and the notations of each case are summarized in Table 2.

4.1. Verification on a simple empty fetch at laboratory scale

In this section, the proposed ABL approach was first verified on simple 2D laboratory scale case namely the neutral homogenous ABL reproduced by the atmospheric wind tunnel for University of Hamburg, (CEDVAL A1-1) (Leitl, 1998), for which velocity and turbulence intensity measurements are available. The 2D domain has the size of 4×1 m and the mesh has 400×71 cells. The mesh is uniform in the longitudinal direction with a cell length of 0.01 m, and it is stretched in the vertical direction with a 6.05 ratio between the last and the first cell, the height of the wall adjacent cell having a size of 0.005 m. The interpolated experimental data of the velocity and turbulent quantities were introduced for boundary condition at inlet and the top boundary, while zero longitudinal gradient is imposed at the outlet. The fitted data at the inlet correspond to a friction velocity as $u_\tau = 0.374\ \mathrm{ms}^{-1}$ and a reference velocity as $U_{ref} = 1.42\ \mathrm{ms}^{-1}$ at $z_{ref} = 1$ m. The fitting parameters for the reformulated turbulent kinetic energy profile are $A_{PB} = -3.82\mathrm{e}{-2}$ and $B_{PB} = 5.15\mathrm{e}{-1}$, while for the Yang profile, $A_{YA} = -4.54\mathrm{e}{-2}$ and $B_{YA} = 2.62\mathrm{e}{-1}$, respectively.

Fig. 1 shows inlet and outlet profiles of velocity, turbulent kinetic energy and dissipation rate. It can be observed that the approach proposed by Parente et al. (2011b) ensured homogeneity of velocity and turbulence between inlet and outlet sections of the domain. Furthermore, it allowed retrieving almost the exact value of the wall shear stress, at difference of the standard wall function reformulated in terms of the aerodynamic roughness.

4.2. Validation on a simplified 3D hill at laboratory scale

For the investigation of the approach on more complex cases, simulations were performed on more complex geometries. The implemented modifications and the new models were tested against the measurements obtained in the thermally stratified wind tunnel of The University of Tokyo, using three-dimensional laser doppler anemometry (Takahashi et al., 2005). The model is an axisymmetric hill, whose shape is defined as Eq. (13), with the radius at the hill base of $r_{max} = 0.42$ m and with the height at the hill-top $h_{max} = 0.2$ m.

$$h(r) = \begin{cases} h_{\max} \frac{1}{2}\left[1 + \cos\frac{2\pi r}{r_{\max}}\right], & \text{if } r < r_{\max} \\ 0, & otherwise \end{cases} \tag{13}$$

The hill model is positioned 2 m downstream of the inlet of the test section of the wind tunnel, which has a size of $6 \times 2.2 \times 1.8$ m. The computational domain contains the entire test section. The origin of the model coordinate system is set to the $x = 0$, $y = 0$ position. The hill and the floor of the wind tunnel are modeled as rough walls with the same physical roughness as $z_0 = 1.22\mathrm{e}{-3}$m, while smooth wall boundary conditions were applied on its ceiling and side walls. At the downwind side, a pressure outlet boundary condition was used. The interpolated experimental data of the velocity and turbulent quantities are introduced at inlet, while zero longitudinal gradient is imposed at the outlet. The fitted data at the inlet correspond to a friction velocity as $u_\tau = 0.0923\ \mathrm{ms}^{-1}$, a boundary layer height as $\delta = 0.67$ m, and a free stream velocity as $U_\infty = 1.42\ \mathrm{ms}^{-1}$. The fitting parameters for the turbulent kinetic energy profile are $A = -0.0053$ and $B = 0.050$ parameters, respectively.

The computational mesh is composed of $200 \times 87 \times 60$ cells, resulting in 1.044 million hexahedral elements refined horizontally at the near-field of the hill. A grid sensitivity analysis was carried out to estimate the solution error associated to the discretization. The investigation was performed using two additional grids with a uniform coarsening ratio ($r = h_2/h_1 = h_3/h_2 = 1.5$) in each coordinate direction, as prescribed by Roache (1998), resulting in 303240 and 93717 cells, respectively. The hit rate for velocity and turbulent kinetic energy measurements was employed as monitoring parameter for the selection of the grid using OpenFOAM. The hit rate was used as a quality assessment metric for the quantitative characterization of the simulations. This quantity indicates the fraction of N measurement locations where the CFD results are within 25% interval of the measurement data (Franke et al., 2007), if the uncertainties of the measurements are not available, such as in our case. The results summarized in

Table 2
Notations for different simulation cases.

Case	Notation	Inlet BC	Wall BC	G_k	C_μ	S_ε	ν_t
Simple empty fetch	C PB	Parente and Benocci (2010)	modified	STD	$C_\mu^{General}$	S_ε	STD
	O YA	Yang et al. (2009)	original	STD	0.09	–	STD
Hills	C	Parente and Benocci (2010)	modified	STD	$C_\mu^{Blended}$	$S_\varepsilon^{Blended}$	STD
	C KL	Parente and Benocci (2010)	modified	KLY	$C_\mu^{Blended}$	$S_\varepsilon^{Blended} + S_\varepsilon^{Yap}$	STD
	C MMK	Parente and Benocci (2010)	modified	STD	$C_\mu^{Blended}$	$S_\varepsilon^{Blended}$	MMK
	O	Richards and Hoxey (1993)	original	STD	0.09	–	STD

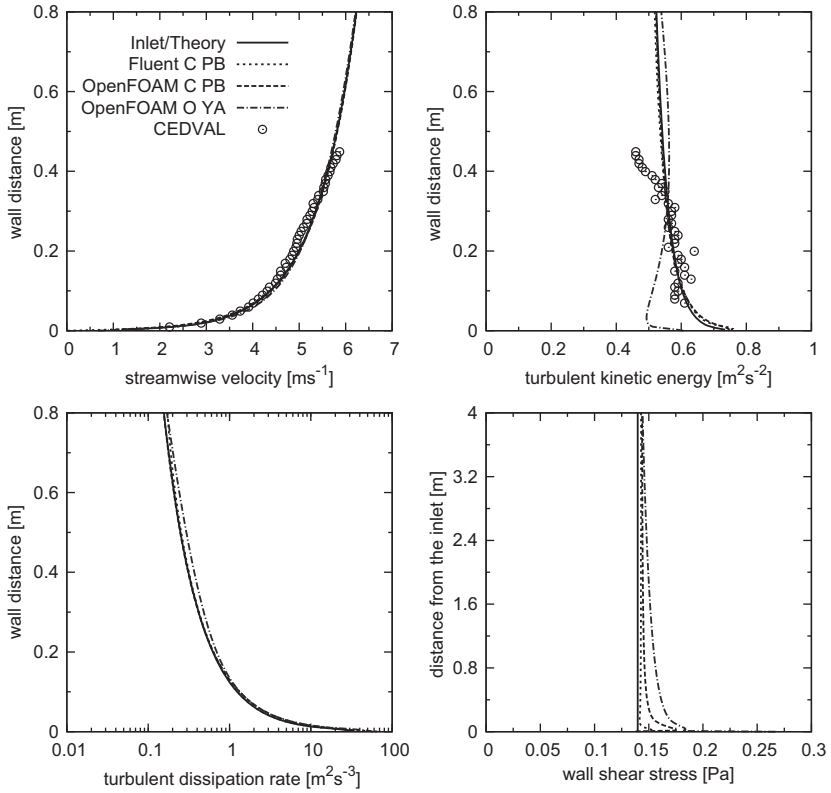

Fig. 1. Inlet and outlet profiles against measurements (CEDVAL data), O—original rough wall function, C—Comprehensive approach, YA—Yang et al. (2009) inlet profiles, PB—Parente et al. (2011b) inlet profiles.

Table 3
Hit rates values for the different meshes on the 3D hill.

Cases	Streamwise velocity [%]	Turbulent kinetic energy [%]
Coarse	76.12	47.47
Medium	81.33	48.56
Fine	79.76	50.93

Table 4
Hit rates values for simulations on the 3D hill.

Cases	Streamwise velocity [%]	Turbulent kinetic energy [%]
OpenFOAM C	81.33	48.56
OpenFOAM C KLY	79.31	41.43
OpenFOAM C MMK	79.31	47.08
OpenFOAM O	68.20	1.08
Fluent C	71.07	47.21
Fluent C KLY	69.04	47.72
Fluent C MMK	69.54	52.28
Fluent O	62.44	4.06

Table 3 indicated a very slight variation of hit rates between the set of meshes; therefore, the medium-size grid was chosen as it provided the best compromise between the computational cost and model accuracy.

Fig. 2 shows the measured and computed velocity and turbulent kinetic energy profiles along the longitudinal direction, provided by the comprehensive approach with a blending exponent $N=3$ using the medium grid with the standard production term for turbulent kinetic energy. The value $N=3$ for the blending exponent was chosen as it provided the best compromise between velocity and turbulent kinetic energy predictions. It can be observed that, for the simulated case, the effect of the turbulence model formulation is not significant for the velocity predictions provided by Fluent, whereas a substantial improvement is observed for OpenFOAM applying the proposed approach, especially for velocity prediction. As far as turbulent kinetic energy is concerned, OpenFOAM simulations always present a large underestimation of k downstream of the hill, whereas Fluent provides calculated values more in agreement with the measurements. However, this effect is due to the large overestimation of the size of the separation bubble by Fluent, which results in erroneous velocity predictions but turbulent kinetic energy levels closer to the measured ones.

A comparison of the wall shear stress as a function of the non-dimensional longitudinal coordinate is given in Fig. 3, where the circles denote the values extracted from measurements. The comparison shows that the simulations are in fair accordance with the observations in the separated region, whereas an important deviation can be remarked at the first measurement location at the top of the hill. The latter can be caused by the difference between the roughness elements mounted on the flat part of the wind tunnel and the hill surface. The wall shear stress obtained by Fluent better reproduces the experimental data, especially as the distance from the hill increases.

The hit rate results presented in Table 4, quantitatively support the conclusion that both the velocity and turbulent kinetic energy prediction is significantly improved by the comprehensive approach.

The computational results consistently show significant differences between OpenFOAM and Fluent, concerning the reproduction of the separation bubble. Table 5 shows that the separation point for all Fluent simulations is far before the measured one and that

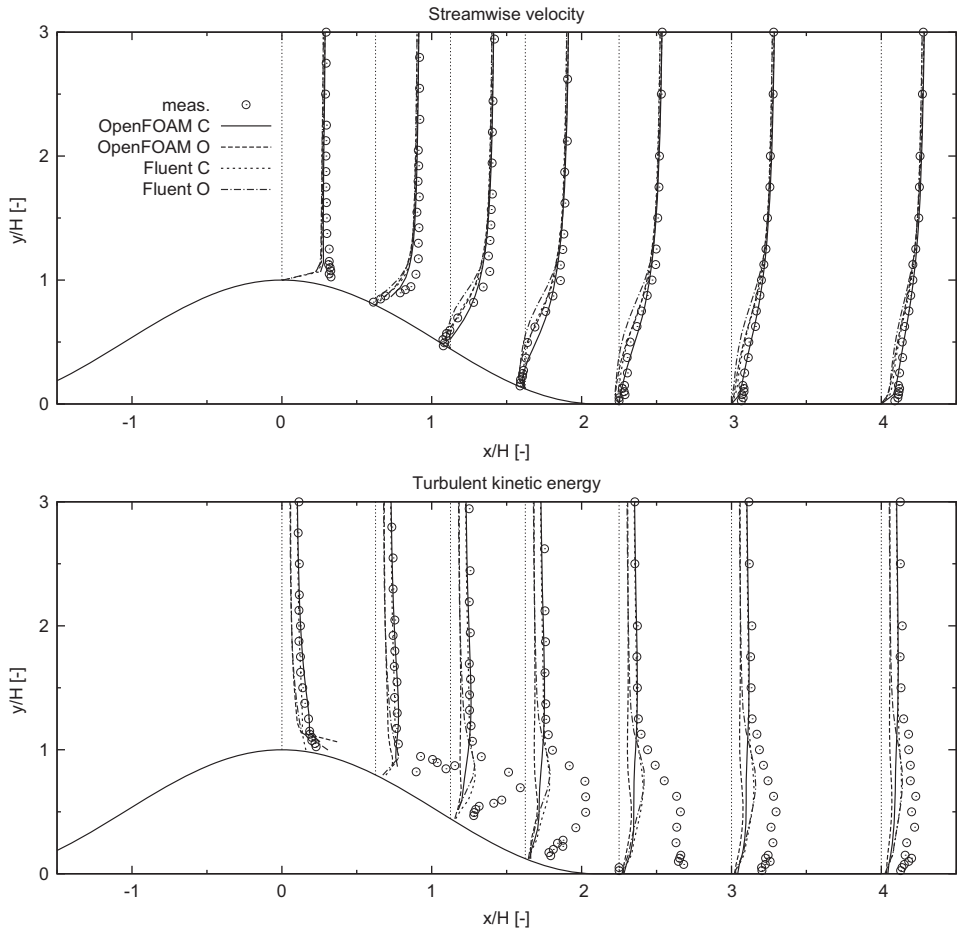

Fig. 2. Streamwise velocity (top) and turbulent kinetic energy profiles (bottom) in the symmetry plane against measurements obtained on the 3D hill at laboratory scale.

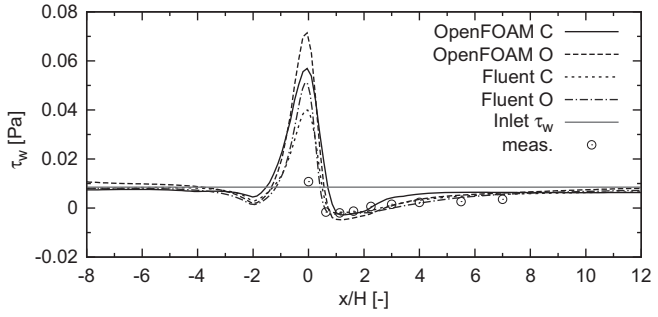

Fig. 3. Simulated wall shear stress along the symmetry of the domain against theoretical values, extracted from the inlet profile (Inlet τ_w) and against values extracted from measured profiles (meas.).

Table 5
Errors on the separation region for the 3D hill, normalized by length of the wake extracted from the measurements. Negative and positive values sign the under- and overestimation respectively.

Case	Normalized error of the separation point location [%]	Normalized error of the wake length [%]
OpenFOAM C	−6.30	−12.53
OpenFOAM C KLY	−6.77	−7.37
OpenFOAM C MMK	−9.01	−5.08
OpenFOAM O	−20.95	36.86
Fluent C	−26.23	28.99
Fluent C KLY	−27.60	39.91
Fluent C MMK	−28.87	32.92
Fluent O	−33.96	65.60

the wake length is consequently overestimated. When the comprehensive approach is applied in OpenFOAM, both the location of the separation point and the size of the wake show a fairly good agreement with the measurements, as indicated by the error values listed in Table 5. The length of the wake is highly affected by the location of the separation point, which is erroneously predicted in Fluent. This can be explained by the differences between turbulence models. While the velocity at the hilltop is quiet similar for OpenFOAM and Fluent (only a few percent difference can be observed), the turbulent kinetic energy near to the surface is overestimated by OpenFOAM and underestimated by Fluent. It is interesting to observe that when the original k-ε model is applied for both solvers, the results are comparable. When the turbulence model modifications are applied, however, the results improve for the OpenFOAM implementation whereas a less pronounced improvement is observed for the Fluent results (Table 5). This can be explained by taking into account that in OpenFOAM full access to the source code is possible whereas in Fluent the modifications are carried out by means of user-defined functions which are "interpreted" by the code. This interpretation step, which is not controllable by the user, is likely to be the cause of the discrepancies between the two codes, being their performances comparable for the base k-epsilon case. While it is difficult to provide a definitive explanation for such discrepancies, it should be recalled that several literature studies (e.g. Bechmann, 2006) has indicated that Fluent solution schemes are generally very dissipative, which can explain the overestimation of the

recirculation region and the differences between Fluent and OpenFOAM.

4.3. Validation on the Askervein hill at full scale

In practical atmospheric applications the surface is generally not as regular as in the previous example; therefore, simulations were performed on more complex geometry to validate the approach and, possibly, propose modifications. In particular, the full scale measurements obtained over the Askervein hill (Taylor and Teunissen, 1983, 1985) were chosen to this purpose. This is a popular case study for validating CFD models for ABL simulations and it was, therefore, investigated formerly by several authors, such as Raithby et al. (1987), Kim and Patel (2000), Castro et al. (2003a, 2003b) and Rodrigues (2005), applying different turbulence models.

The Askervein hill has a nearly elliptical form with major and minor axis of 2000 and 1000 m. The height of the hill is 116 m, and its slopes range from 12 to 25%. The surrounding area is flat at the upwind side of the hill, and it is hilly at the downwind side. For describing the surface coverage, the aerodynamic roughness was taken as $z_0=3.53e-2m$, based on the data measured at the reference mast. The computational domain (Fig. 4) has dimensions $6000\times6000\times1000$ m with an origin located at the hill top (HT). Similarly to a previous study (Rodrigues, 2005), the mesh was generated with $97\times111\times30$ hexahedral elements using 15 m maximum resolution on the hill and 1 m for the first cell height. The refinement the grid at the hill is shown in Fig. 4. Assuming that the terrain does not affect the flow on the top of the domain, the same velocity inlet boundary condition was used as in the inlet, defining U, k, and ε. At the downwind side of the domain pressure outlet and at the lateral sides of the domain symmetry boundary condition was used.

Measurements had been obtained at almost neutral condition, stable wind direction and relatively high wind speed (Mickle et al., 1988). The wind direction was 210 degrees, which determines the mesh orientation. Namely, the inlet is fixed on the western side of the computational domain and the outlet is the eastern side. On its southern and northern side the symmetry boundary condition are defined. On the top of the domain, the uniform values, corresponding to the fitted profiles are imposed. The profile fitting is based on the data of Mickle et al. (1988). They correspond to $u_\tau=0.661$ ms^{-1} and $U_{ref}=9.11$ ms^{-1} at $z=10$ m at the inlet. The fitting parameters (Section 2.2) for the definition of inlet quantities are: $A=-0.351$ and $B=2.61$. The wall treatments and modifications are equivalent to the simulation of the simplified 3D hill.

The measurement campaign was carried out using sonic anemometers at 10 m above the surface, in every must along a given line (denoted as line-A in Fig. 4) and at the hill top, thus the velocity components, such as the turbulent fluctuations for the three directions are available for these locations. The comparison between computed and measured horizontal profiles is shown in Fig. 5: the horizontal component (U_h), vertical velocity (W) and turbulent kinetic energy are presented, where the RMS of the velocity is used to characterize the uncertainty.

The agreement between measured and computed velocity can be considered sufficiently satisfactory. Although the comprehensive approach overestimates the horizontal velocity at the far upwind of the hill summit (19.4% for OpenFOAM and 12.1% for Fluent), its prediction at the top of the hill (Figs. 5 and 6) and along the downwind of the hill is fairly good (underestimation of 2.1% for OpenFOAM and 5.5% for Fluent). The simulation using the original approach provides also good agreement, especially in the far upwind area, although the agreement is worse at the top of the hill and in the downwind region. As for turbulent kinetic energy, the results obtained with the comprehensive approach are significantly better than the ones given by the original approach, even at the top of the hill.

The differences between the CFD solvers are significant: OpenFOAM results are better for velocity, whereas Fluent provides a more accurate prediction of turbulent kinetic energy. Table 6 shows the hit rate of the horizontal velocity and the turbulent kinetic energy for the OpenFOAM and Fluent codes, furthermore the relative errors of the fractional speed-up ratio (FSR) at 30 m above the ground. This latter quantity characterizes the acceleration effects of the terrain as the increment of the velocity: $FSR=(U-U_0)/U_0$, where U is the velocity at a given level, while U_0 the undisturbed velocity at the same level. A hit-rate value of 100% for velocity is obtained for the OpenFOAM simulation using the comprehensive approach with the MMK model, with a corresponding hit rate of about 44% for turbulent kinetic energy. A higher HR value for k is obtained only using Fluent in combination with the Kato-Launder correction. However, for this case, the hit-rate value for velocity is far below 100%, i.e. 81%. The relative errors of FSR shows, that OpenFOAM could be an effective tool for wind turbine sitting.

In general, the comprehensive approach affects the performances of both codes for the full-scale simulations; the single exception of the velocity predictions provided by Fluent.

4.4. Computational performances

To have a complete comparison between the Fluent and OpenFOAM solvers, the computational costs of the calculations are monitored. The calculations are executed on the same computer and platform, namely on one core of an Intel Core 2 Quad computer

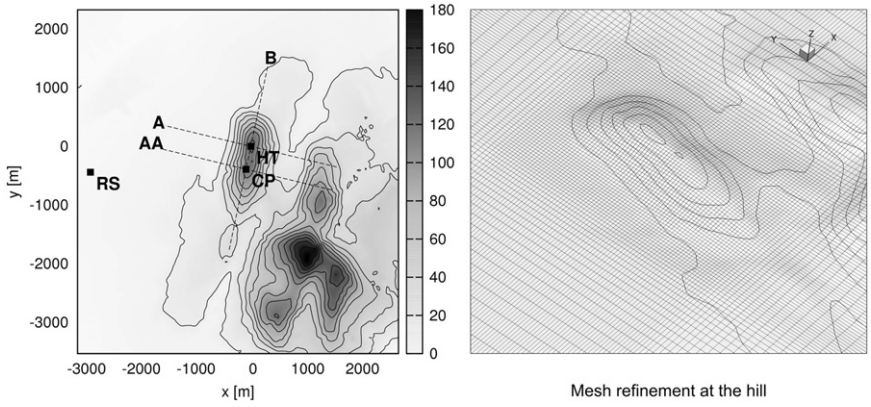

Fig. 4. Domain around the Askervein hill (left) shaded by the terrain elevation and the computational mesh refined at the hill (right).

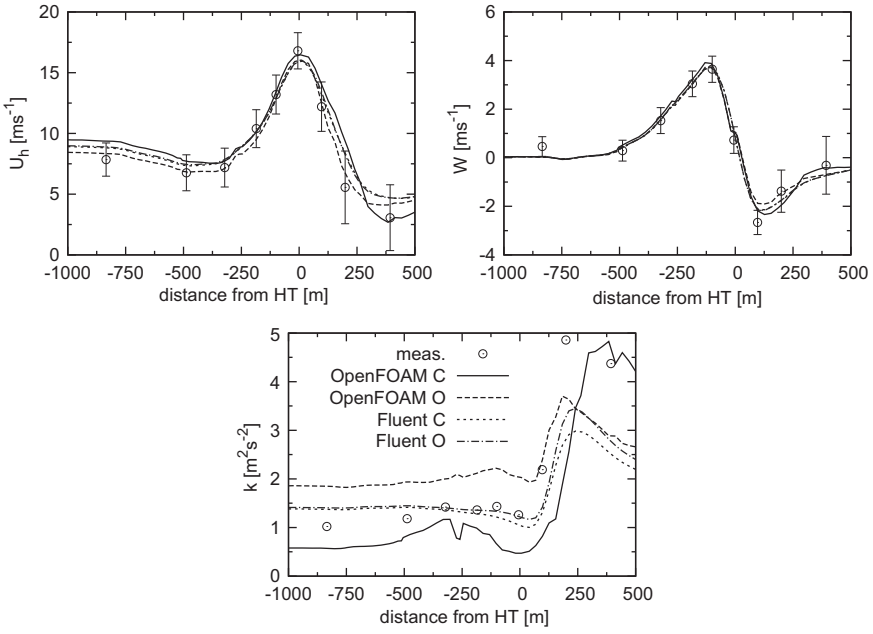

Fig. 5. Comparison of simulated and measured horizontal and vertical stream velocity (U_h and W), and turbulent kinetic energy (k) along line-A. Notations: C–comprehensive approach ($N=3$) using PB inlet profiles, O—modified rough wall formulation using RH inlet profiles.

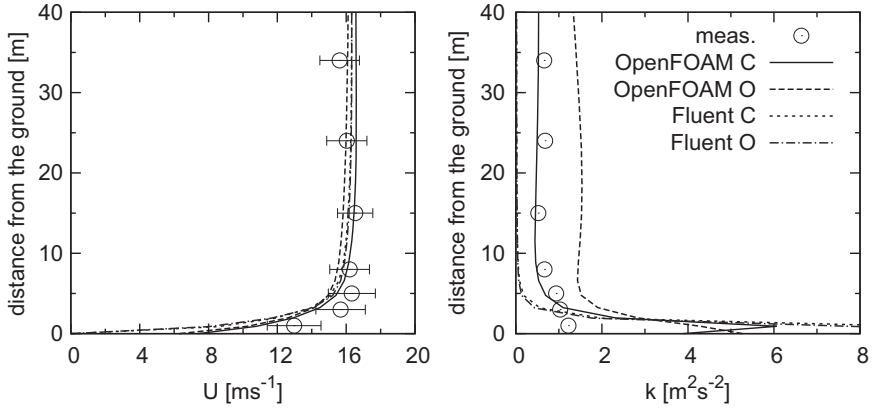

Fig. 6. Comparison of simulated and measured vertical profiles (U and k), at the hill summit (HT).

Table 6
Hit rates and relative errors on fractional speed-up ratio for simulations on the Askervein hill.

Case	Hit rate on U_h [%]	Hit rate on k [%]	Relative error on FSR at 30 m [%]
OpenFOAM C	93.75	31.25	5.38
OpenFOAM C KLY	93.75	25.00	3.42
OpenFOAM C MMK	100.00	43.75	4.31
OpenFOAM O	87.50	12.50	−4.41
Fluent C	81.25	43.75	8.83
Fluent C KLY	81.25	50.00	8.71
Fluent C MMK	81.25	43.75	7.31
Fluent O	81.25	37.50	9.54

(Q6600 3 GHz, 8 GB RAM). Due to convergence problems observed in Fluent, the numerical setup was different. Although in OpenFOAM the simple velocity-pressure coupling was used, at difference of to the coupled scheme used in Fluent, the time requirements of the simulations were quite similar (Table 7). However, the memory usage is two times higher for Fluent (~1.37 Gb on Askervein and ~1.5 Gb on the 3D hill) than for OpenFOAM (~660 Mb on Askervein and ~780 Mb on the 3D hill), due to the higher memory allocation related to the coupled solver. Surprisingly, at full scale, the comprehensive approach converged faster than the original approach, for both solvers.

5. Conclusions

A recent approach for the simulation of the neutral ABL was applied for the simulation of flows over complex terrains. The approach was implemented in OpenFOAM and validated against experimental data obtained on different cases with varying complexity a 2D empty fetch, a 3D sinusoidal hill at wind tunnel scale and the full-scale Askervein Hill. The results indicate the potential of the proposed approach for the numerical simulation of ABL flows over complex terrains. In particular, the validation study on the 3D cases pointed out the major influence of appropriate inlet and wall conditions on the results. Moreover, the impact of turbulence model corrections, i.e. Kato-Launder and Yap appeared to be relevant for full-scale simulations. In general the results indicate satisfactory predictions for velocity, with hit rate values around 80%, whereas the performances of the model

Table 7
Computational performances (time in seconds/number of steps is needed for full convergence).

Case	3D hill (lab. scale)	Askervein (full scale)
OpenFOAM C	12367/2000	5093/500
OpenFOAM C KLY	18999/2000	5892/500
OpenFOAM C MMK	12738/2000	5548/500
OpenFOAM O	18008/2000	5204/500
Fluent C	14451/2000	4947/500
Fluent C KLY	21254/2000	5075/500
Fluent C MMK	18418/2000	4506/500
Fluent O	20881/2000	5209/500

for turbulent kinetic energy appears inadequate, being the highest obtained hit rate values for k equal to 50%. This trend is observed for all the simulated cases, codes and modification of k-ε leads, which indicate an intrinsic limitation of linear k-ε. Therefore, the implementation of non-linear k-ε turbulence model is currently under investigation, as it could have the potential of better performing in the recirculation zones of the flow, as it is reported by different authors such as Papageorgakis and Assanis (1999) and Lun et al. (2003).

The successful implementation of the present model proves its flexibility and generality. The OpenFOAM toolbox proved to be a very useful tool for ABL flows; compared with an available commercial code, it yielded better results with comparable numerical effort and even better performance in memory requirements.

Acknowledgments

The first author was supported by the Von Karman Institute (VKI) during the academic year 2009–2010 in the frame of Research Master in Fluid Dynamics program. We would like to express our gratitude to Dr. Takahashi and to the University of Tokyo for the experimental data concerning the wind-tunnel investigation of Takahashi et al. (2005).

References

Bechmann, A., 2006. Large-Eddy Simulation of Atmospheric Flow over Complex Terrain. Ph. D. Thesis, Technical University of Denmark.
Bechmann, A., Berg, J., Courtney, M., Mann, J., and Sørensen, N.N., 2009. The Bolund experiment: Blind Comparison of CFD codes—Wind in Complex Terrain. Technical report.
Blocken, B., Stathopoulos, T., Carmeliet, J., 2007a. CFD evaluation of wind speed conditions in passages between parallel buildings—effect of wall-function roughness modifications for the atmospheric boundary layer flow. Journal of Wind Engineering and Industrial Aerodynamics 95, 941–962.
Blocken, B., Stathopoulos, T., Carmeliet, J., 2007b. CFD simulation of the atmospheric boundary layer: wall function problems. Atmospheric Environment 41, 238–252.
Castro, F.A., Palma, J.M.L.M., Silva Lopes, A., 2003a. Simulation of the askervein flow. part 1: Reynolds averaged navier-stokes equations (k-ε turbulence model). Boundary-Layer Meteorology 107/3, 501–530.
Castro, F.A., Palma, J.M.L.M., Silva Lopes, A., 2003b. Simulation of the askervein flow. part 2: Large-eddy simulations. Boundary-Layer Meteorology 125/1, 85–108.
Crasto, G., 2007. Numerical Simulations of the Atmospheric Boundary Layer. Ph. D. Thesis, University of Cagliari.
Dejoan, A., Santiago, J.L., Martilli, A., Martin, F., Pinelli, A., 2010. Comparison between LES and RANS computations for the MUST field experiment. Part II: Effects of incident wind angle deviation on the mean flow and plume dispersion. Boundary-Layer Meteorology 135, 133–150.
Donat, J., 1995. Wind kanal experimente zur Ausbreitung von Schwergas-strahlen. Ph. D. Thesis in the University of Hamburg, Meteorological Institute.
Franke, J., Hellsten, A., Schlunzen, H., Carissimo, B., 2007. Best Practice Guideline for the CFD Simulation of Flows in the Urban Environment, COST Action 732.
Gorlé, C., Van Beeck, J., Rambaud, P., Van Tendeloo, G., 2009. CFD modelling of small particle dispersion: The influence of the turbulence kinetic energy in the atmospheric boundary layer. Atmospheric Environment 43, 673–681.
Gorlé, C., Van Beeck, J., Rambaud, P., 2010. Dispersion in the wake of a rectangular building: validation of two Reynolds-averaged Navier–Stokes modelling approaches. Boundary-Layer Meteorology 137/1, 115–133.
Hargreaves, D.M., Wright, N.G., 2007. On the use of the k-ε model in commercial CFD software to model the neutral atmospheric boundary layer. Journal of Wind Engineering and Industrial Aerodynamics 95, 355–369.
Kim, H., Patel, V., 2000. Test of turbulence models for wind flow over terrain with separation and recirculation. Boundary-Layer Meteorology 94, 5–21.
Launder, B.E., 1993. Modeling convective heat transfer in complex turbulent flows. In: Proceedings of the Second International Symposium.
Launder, B.E. and Kato, M., 1993. Modeling flow-induced oscillations in turbulent flow around a square cylinder. In: ASME Fluid Engineering Conference.
Leitl, B.,1998. Cedval at Hamburg University. 〈http://www.mi.uni-hamburg.de/Introducti.433.0.html〉 (accessed in January 2010).
Lim, H., Thomas, T., Castro, I.P., 2009. Flow around a cube in a turbulent boundary layer: LES and experiment. Journal of Wind Engineering and Industrial Aerodynamics 97, 96–109.
Lun, Y.F., Mochida, A., Murakami, S., Yoshino, H., Shirasawa, T., 2003. Numerical simulation of flow over topographic features by revised k-ε models. Journal of Wind Engineering and Industrial Aerodynamics 91, 231–245.
Mickle, R.E., Cook, N.J., Hoff, A.M., Jensen, N.O., Salmon, J.R., Taylor, P.A., Tetzlaff, G., Teunissen, H.W., 1988. The Askervein Hill project: Vertical profiles of wind and turbulence. Boundary-Layer Meteorology 43, 143–169.
Papageorgakis, G.C., Assanis, D.N., 1999. Comparison of linear and non-linear RNG-based k-epsilon models for incompressible turbulent flows. Numerical Heat Transfer, Part B 35, 1–22.
Parente, A., Gorlé, C., van Beeck, J., Benocci, C., 2011a. Improved k-ε model and wall function formulation for the RANS simulation of ABL flows. Journal of Wind Engineering and Industrial Aerodynamics 99, 267–278.
Parente, A., Benocci, C., 2010. On the RANS simulation of neutral ABL flows. In: Proceedings of the Fifth International Symposium on Computational Wind Engineering (CWE2010) Chapel Hill, North Carolina, USA, May 23–27, pp. 1–8.
Parente, A., Gorlé, C., van Beeck, J., Benocci, C., 2011b. A comprehensive modelling approach for the neutral atmospheric boundary layer: consistent inflow conditions, wall function and turbulence model closure. Boundary-Layer Meteorology 140/3, 411–428.
Pontiggia, M., Derudi, M., Rota, R., 2009. Hazardous gas dispersion: A CFD model accounting for atmospheric stability classes. Journal of Hazardous Materials 171 (1–3), 739–747.
Raithby, G.D., Stubley, G.D., Taylor, P.A., 1987. The Askervein hill project: A finite control volume prediction on three-dimensional flows over the hill. Boundary-Layer Meteorology 39, 107–132.
Richards, P.J., Hoxey, R., 1993. Appropriate boundary conditions for computational wind engineering models using the k—ε turbulence model. Journal of Wind Engineering and Industrial Aerodynamics 47, 145–153.
Riddle, A., Carruthers, D., Sharpe, A., McHugh, C., Stocker, J., 2004. Comparisons between FLUENT and ADMS for atmospheric dispersion modelling. Atmospheric Environment 38, 1029–1038.
Roache, P.J., 1998. Verification and validation in computational science and engineering. Hermosa Publishers, Albuquerque, NM 464p.
Rodi, W., 1997. Comparison of LES and RANS calculations of the flow around bluff bodies. Journal of Wind Engineering and Industrial Aerodynamics 69–71, 55–75.
Rodrigues, C.A.V., 2005. Analysis of the atmospheric boundary layer flow over mountainous terrain. Master's Thesis, von Karman Institute for Fluid Dynamics.
Shah, K., Ferziger, J., 1997. A fluid mechanicians view of wind engineering: large eddy simulation of flow past a cubic obstacle. Journal of Wind Engineering and Industrial Aerodynamics 67–68, 211–224.
Takahashi, T., Kato, S., Murakami, S., Ooka, R., Yassinc Mohamed Fassy, M., Kono, R., 2005. Wind tunnel tests of effects of atmospheric stability on turbulent flow over a three-dimensional hill. Journal of Wind Engineering and Industrial Aerodynamics 93, 155–169.
Taylor, P.A., Teunissen, H.W., 1983. Askervein '82: Report on the September/October 1982 experiment to study boundary layer flow over Askervein. Technical Report MSRS-83-8, Meteorological Services Research Branch Atmospheric Environment Service.
Taylor, P.A., Teunissen, H.W., 1985. The Askervein Hill project: Report on the September/October 1983, main field experiment. Technical Report MSRB-84-6, Meteorological Services Research Branch Atmospheric Environment Service.
Tsuchiya, M., Murakami, S., Mochida, A., Kondo, K., Ishida, Y., 1997. Development of a new k—ε model for flow and pressure fields around bluff body. Journal of Wind Engineering and Industrial Aerodynamics 67–68, 169–182.
Xie, Z., Castro, I.P., 2006. LES and RANS for turbulent flow over arrays of wall-mounted obstacles. Flow, Turbulence and Combustion 76, 291–312.
Yap, C.J., 1987. Turbulent Heat and Momentum Transfer in Recirculating and Impinging Flows. Ph.D. Thesis. University of Manchester.
Yang, Yi., Gu, M., Chen, S., Jin, X., 2009. New inflow boundary conditions for modeling the neutral equilibrium atmospheric boundary layer in computational wind engineering. Journal of Wind Engineering and Industrial Aerodynamics 97, 88–95.